Fluorescence Excitation and Hole-Burning Spectra of Jet-Cooled Tropolone−M (M = N_2, CO) van der Waals Complexes: Structures and Proton Tunneling in the S_1 State

Hidenori Hamabe,[†] Tetsuro Fukuchi,[‡] Sakaki Shiraishi,[‡] Kaori Nishi,[‡] Yukio Nishimura,*[,†] Takeshi Tsuji,[†] Nobuyuki Nishi,[‡,§] and Hiroshi Sekiya*[,‡]

Institute of Advanced Material Study and Department of Molecular Science and Technology, Graduate School of Engineering Sciences, Kyushu University, Kasuga-shi, Fukuoka 816-8580, Japan, and Department of Chemistry, Faculty of Science, Kyushu University, Hakozaki, Higashi-ku, Fukuoka 812-8581, Japan

Received: December 4, 1997; In Final Form: February 18, 1998

Proton tunneling in the S_1 state of jet-cooled tropolone−$(N_2)_n$ ($n = 1, 2$) and tropolone−$(CO)_1$ van der Waals complexes is investigated by measuring the hole-burning and fluorescence excitation spectra in the S_1-S_0 region. The hole-burning spectra enabled us to separate three overlapping absorption systems due to transitions between low-wavenumber and high-wavenumber tunneling doublet components of tropolone−$(N_2)_1$ and those of tropolone−$(N_2)_2$. The 0−0 tunneling doublet splitting of tropolone−$(N_2)_1$ has been confirmed to be 9.7 cm^{-1}. It has been suggested that the magnitude of the tunneling splitting depends on the excited intermolecular vibrational level. In addition to the sandwich isomer I for tropolone−$(N_2)_2$ observed previously, a second isomer [II] has been identified. A much smaller microscopic red shift (−57.9 cm^{-1}) than the corresponding value (−129.0 cm^{-1}) for isomer I indicates that two N_2 molecules are on the same side of the tropolone ring in isomer II. No tunneling splitting has been observed for tropolone−$(N_2)_2$[II]. The hole-burning spectrum of tropolone−$(CO)_1$ indicates that only one species is observed in the excitation spectrum, although the existence of two isomers was reported previously (*Chem. Phys*. **1996**, *213*, 397). The vibronic bands of tropolone−$(CO)_1$ show no tunneling splitting. The intensity of the origin band of tropolone−$(CO)_1$ is considerably weaker than vibronic bands, suggesting that the equilibrium structure in the S_1 state is substantially different from that in the S_0 state. The decreases in the tunneling splittings of tropolone−$(N_2)_n$ ($n = 1, 2$) and tropolone−$(CO)_1$ are attributed to the coupling of the intermolecular vibrations with intramolecular vibrations, which may significantly increase the height of the potential energy barrier and distort the potential energy surface in the S_1 state, leading to the decreased tunneling splitting. This coupling is very strong when the adduct is bonded close to the O···H−O moiety.

1. Introduction

Tropolone (TRN) is one of the most extensively studied polyatomic molecules that exhibit symmetric proton transfer through the potential energy barrier. The displacements of all the nuclei in the molecule are involved in the tunneling process. Therefore, the tunneling potential energy surfaces (PESs) should be described by using multidimensional coordinates. Tropolone is an excellent model system for studying multidimensional tunneling in the isolated state, because TRN is volatile and emits strong fluorescence. In addition, the tunneling splittings of vibronic levels in the S_1 state of TRN are easy to measure due to moderate separations between the two tunneling doublet components. A lot of experimental and theoretical studies have been carried out to investigate the proton tunneling dynamics in TRN.[1−12]

We noted that the tunneling splittings measured in the isolated state and those in the low-temperature rare gas matrixes are significantly different. For example, the tunneling splittings of the S_1-S_0 (0−0) transition of TRN(OH) and TRN(OD) measured in a neon matrix are 21 and 7 cm^{-1}, respectively,[1] while the corresponding values are 18.9 and 2.2 cm^{-1} in the isolated state.[2] The difference in the tunneling splitting may be attributed to the effects of the crystal field, which induces asymmetry in the double-minimum potential well. 9-Hydroxyphenalenone is also a typical organic molecule that exhibits the effects of proton tunneling in the electronic spectrum.[13−17] The electronically forbidden 0^-_+ and 0^+_- transitions were observed in the excitation spectra of 9-hydroxyphenalenone and its OD species in rare gas matrixes,[13−17] which provided evidence of asymmetry in the double-minimum potential wells in the S_0 and S_1 states of 9-hydroxyphenalenone.

The results of TRN and 9-hydroxyphenalenone indicate that proton tunneling is very sensitive to the perturbations from surrounding atoms or molecules. The sensitivity of proton tunneling due to intermolecular interactions prompted us to investigate the effects of solvation on proton tunneling by synthesizing van der Waals (vdW) complexes containing TRN as a chromophore in a supersonic jet. The measurement of the excitation spectra of the vdW complexes may provide information about the effects of perturbations from surrounding molecules on proton tunneling in the isolated state. The attachment of an atom or a molecule to TRN gives additional coordinates. The effects of well-defined coordinates on proton tunneling can be obtained by measuring the tunneling doublet

* Author to whom correspondence should be addressed.
[†] Institute of Advanced Material Study and Graduate School of Engineering Sciences.
[‡] Faculty of Science.
[§] Present address: Institute for Molecular Science, Myodaiji, Okazaki-shi 444, Japan.

S1089-5639(98)00418-6 CCC: $15.00
Published on Web 05/08/1998

splittings. Such information is important to investigate the difference in the proton tunneling between the gas phase and the condensed phase and to understand proton tunneling in solution and biological systems.[18] It is easy to observe vibrationally resolved spectra of jet-cooled van der Waals (vdW) complexes, which enables us to measure the tunneling splittings of vibrationally excited levels as well as the splitting of the zero-point level. We have reported the tunneling splittings of various jet-cooled TRN(OH)−M_n (n = 1, 2) (M = Ar, Kr, Xe, CH_4/CD_4, N_2, C_2H_6, C_3H_8, CCl_4) van der Waals complexes and their deuterated species.[19−21] It has been found that the magnitude of the tunneling splitting significantly depends on both the adduct and the number of adducts.[21]

The molecular polarizability of N_2 (1.76 Å^3) is similar to that of Ar (1.66 Å^3),[22] and the binding energies for TRN(OH)−$(N_2)_1$ and TRN(OH)−Ar_1 are expected to be similar to one another. The 0_0^0 tunneling splitting of TRN(OH)−N_2 (9.7 cm^{-1}) is much smaller than the value (18.9 cm^{-1}) of TRN(OH), while the corresponding splitting of TRN(OH)−Ar_1 (18.6 cm^{-1}) is very similar to that of TRN(OH).[21] The structure of the N_2 molecule is much simpler than the other adducts such as C_2H_6 and C_3H_8 studied previously;[21] therefore, the vibrational analysis of the vdW modes and the prediction of the structures for TRN(OH)−$(N_2)_n$ from theoretical calculations are expected to be easier. The TRN(OH)−$(N_2)_n$ (n = 1, 2, ...) complexes are considered to be an excellent model system to investigate proton tunneling in the vdW complex. Our group and Shinha and Steer reported the fluorescence excitation spectrum of jet-cooled TRN(OH)−N_2. The 0_0^0 tunneling splitting of TRN(OH)−$(N_2)_1$ determined by Sinha and Steer[23] is 6 cm^{-1}, inconsistent with our value of 9.7 cm^{-1}.

The fluorescence excitation spectra of TRN(OH/OD)−$(CO)_n$ (n = 1, 2) were measured very recently.[24] The molecular polarizability of the CO molecule is anisotropic (α = 2.60 Å^3, α = 1.625 Å^3), and the average polarizability (1.95 Å^3) is slightly larger than that of N_2. The CO molecule is isoelectronic with N_2, but the CO molecule is weakly dipolar (0.11 D) and more strongly interacts with TRN than N_2. Two isomers were reported for the 1:1 complex by Sinha et al.[24] The conformation of an isomer TRN−$(CO)_1$ [I] is very similar to the 1:1 complex of TRN−N_2, in which N_2 is located above the molecular plane of TRN(OH), whereas the structure of a second isomer TRN(OH)−$(CO)_1$ [II] was concluded to be very different from that of isomer I; an intermolecular hydrogen bond exists between the hydroxy proton and the carbonyl oxygen of CO.[24] The 0_0^0 tunneling splittings of isomers I and II are determined to be 3.5 cm^{-1} and less than 1 cm^{-1}, respectively. The excitation spectrum of TRN−$(CO)_1$ [II] could be compared to the spectrum of TRN(OH)−$(CH_3COCH_3)_1$, since an intermolecular hydrogen bond may exist between the carbonyl oxygen atom of CH_3COCH_3 and the hydroxy proton. We measured the fluorescence excitation and two-color resonance-enhanced multiphoton ionization spectra of TRN(OH)−$(CH_3COCH_3)_1$.[25] The electronic origin band of the TRN(OH)−$(CH_3COCH_3)_1$ complex was observed at 242 cm^{-1} blue-shifted from the origin band of TRN(OH). If TRN(OH)−$(CO)_1$ has an intermolecular hydrogen bond, the transition energy will be blue-shifted. But the origin of TRN(OH)−$(CO)_1$ [II] is red-shifted from that of the bare molecule.[24] Thus, further studies are needed to conclude the existence of the two isomers for TRN(OH)−$(CO)_1$.

In the present work, we focused on the effects of solvation of two anisotropic molecules, N_2 and CO, on proton tunneling in the S_1 state of TRN(OH). We observed that the mass-selected resonance-enhanced two-photon ionization technique was not useful to identify the cluster size of TRN−M_n, because very fast dissociation of the solvent molecules after ionization prevents mass selection. Hole-burning spectroscopy has been successfully applied to distinguish the transitions between the lower-wavenumber tunneling doublet components and those between the higher-wavenumber ones (H_1^1) as well as to separate the transitions of the isomers. The experimental vibronic patterns, microscopic spectral shifts, and calculated minimum energy structures for TRN(OH)−$(N_2)_n$ (n = 1, 2) are compared with those for TRN(OH)−$(CO)_1$ to obtain information on the tunneling dynamics. The assignments of vibronic bands and the magnitude of the tunneling splittings in previous publications[23,24] have been extensively revised. The structures of the observed complexes and the origin of the quenching of the tunneling splitting have been discussed.

2. Experimental Section

The measurement of the excitation spectrum was carried out by using two apparatuses at the Institute of Advanced Material Study, Kyushu University, and at the Department of Chemistry, Faculty of Science, Kyushu University. The experimental apparatus used at the Institute of Advanced Material Study was essentially the same as that used previously.[19−21] We describe briefly the apparatus at the Department of Chemistry. The vacuum chamber was evacuated by a 10 in. diffusion pump backed by a 1200 L/min oil rotary pump. The nozzle housing was heated to 100 °C with a coiled heater to obtain sufficient vapor pressure for the measurement of the excitation spectrum. The N_2 or CO gas was diluted with the helium carrier gas in a vessel, which was mixed with vaporized TRN(OH) and expanded into the chamber with a pulsed nozzle (General Valve, D = 0.5 mm). The backing pressure of He (P_0) was 2−5 atm, and the partial pressures of N_2 or CO were estimated to be 1−10 Torr. The van der Waals complexes produced in a free jet were probed with a XeCl excimer laser pumped dye laser (Lumonics HE700 and HD300). Total fluorescence was detected with a photomultiplier (Hamamatsu 1P28A), while scanning the wavelength of the dye laser to measure the excitation spectrum. The photocurrent signal was averaged with a digital storage scope (LeCroy 9400). The frequency-doubled output of the idler light of a MOPO system (Spectra Physics) was used for the probe laser, while the output of the dye laser system (Lumonics HE700 and HD300) was employed for the pump laser to obtain the hole-burning spectrum. The two beams were irradiated on the molecular beam from the opposite directions. The beam of the probe laser was unfocused, while that of the pump laser was mildly focused. A typical time delay between the pump and probe lasers was 300 ns. The fluorescence-dip signal was detected with a photomultiplier and averaged with a storagescope while scanning the wavelength of the probe laser.

3. Results

A. Fluorescence Excitation Spectrum of TRN−$(N_2)_n$ (n = 1, 2). Figure 1 shows the fluorescence excitation spectra of TRN(OH)−N_2 measured at relatively lower, medium, and higher partial pressures of N_2, respectively. The top figure is similar to those reported in previous publications.[21,23] The 0_0^0 band of the 1:1 complex is observed at $\Delta\nu$ = −63.8 cm^{-1} (ν = 26953.9 cm^{-1}); here $\Delta\nu$ represents the microscopic red-shift of a vibronic band from the 0_0^0 band of TRN(OH). The peak at $\Delta\nu$ = −129.0 cm^{-1} (ν = 26888.7 cm^{-1}) was assigned to the 0_0^0 transition of the 1:2 complex TRN(OH)−$(N_2)_2$ [I], since the magnitude of the red-shift (−129.0 cm^{-1}) is almost twice that

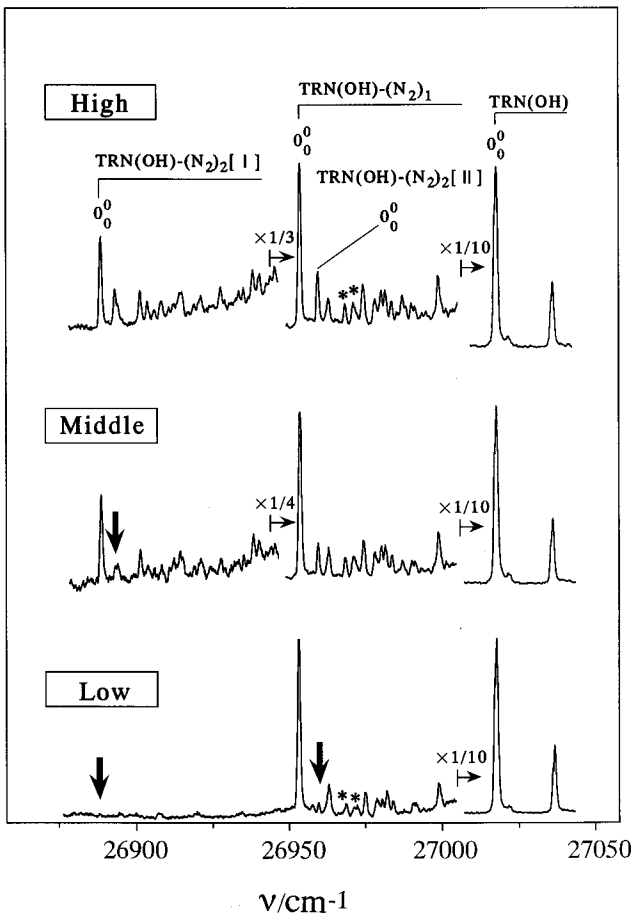

Figure 1. Fluorescence excitation spectra of TRN(OH)−N_2 measured at the higher (a), medium (b), and lower (c) N_2 partial pressures. The experimental conditions were $P_0 = 3.5$ atm, X/D = 80. The intensities of the bands marked by the arrows significantly decreased by decreasing the partial pressure of N_2. The asterisks indicate bands due to TRN-(OH)−$(N_2)_2$ [II], which are overlapping with the bands of the 1:1 complex.

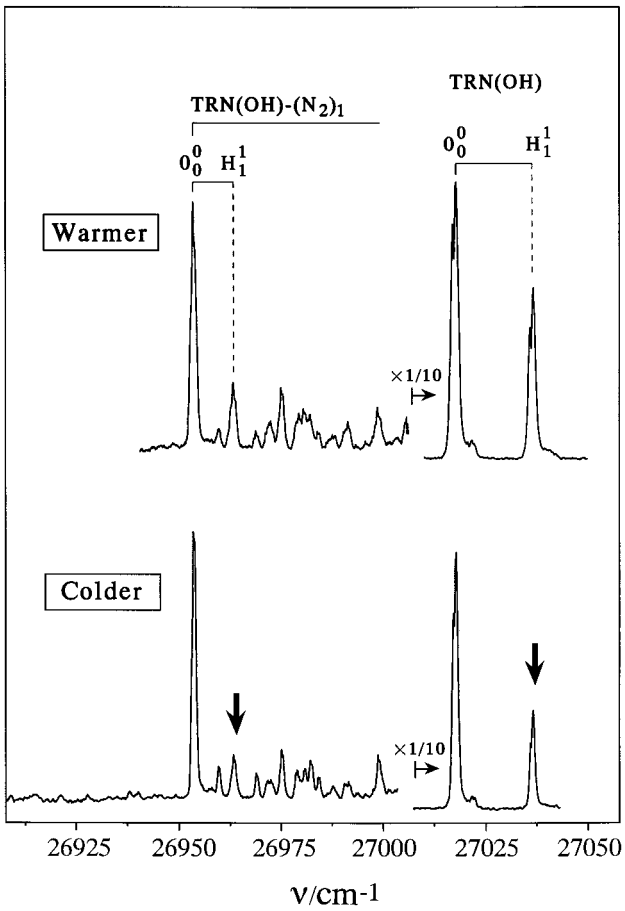

Figure 2. Fluorescence excitation spectra of TRN(OH)−N_2. The intensities of the bands indicated by the arrows decreased significantly under colder conditions. The experimental conditions were $P_0 = 3.5$ atm, X/D = 40 and $P_0 = 3.5$ atm, X/D = 80 for the upper and lower spectra, respectively.

of the 0_0^0 transition of the 1:1 complex, indicating that two N_2 molecules occupy almost equivalent positions; that is, two N_2 molecules are on opposite sides of the plane of TRN(OH). These results are consistent with those in previous publications.[22−24]

It should be noted that the intensity of the band at $\Delta\nu = -57.9$ cm^{-1} ($\nu = 26959.8$ cm^{-1}), which had been assigned to the 0_0^0 H_1^1 transition of the 1:1 complex by Sinha and Steer,[21,23] decreased with decreasing the partial pressure of N_2. This pressure dependence of the intensity of the band at $\Delta\nu = -57.9$ cm^{-1} is very similar to the behavior of the 0_0^0 band of TRN-(OH)−$(N_2)_2$ [I], indicating that the band at $\Delta\nu = -57.9$ cm^{-1} is not a vibronic band of TRN(OH)−$(N_2)_1$, although this band is blue-shifted only 5.9 cm^{-1} from the 0_0^0 band of the 1:1 complex. The band at $\Delta\nu = -57.9$ cm^{-1} must be due to a larger complex. We have assigned this band to the 0_0^0 band of a second isomer of the 1: 2 complex TRN(OH)−$(N_2)_2$ [II]. The bands at $\Delta\nu = -48.6$ and -45.3 cm^{-1} also exhibit a pressure dependence similar to TRN(OH)−$(N_2)_2$ [II] and are assigned to the vdW modes of TRN(OH)−$(N_2)_2$ [II], though vibronic bands of TRN(OH)−$(N_2)_1$ [I] are overlapped with the bands of TRN(OH)−$(N_2)_2$ [II].

The temperature dependence of the intensity of vibronic bands of TRN(OH)−$(N_2)_1$ was measured as functions of the backing pressure (P_0) and the distance (X) between the nozzle and the laser beam. Figure 2 shows the fluorescence excitation spectra of TRN(OH)−$(N_2)_1$ measured under the colder and warmer expansion conditions, respectively. One can obtain qualitative information on the changes in the temperature of the jet by monitoring the intensity ratio $0_0^0H_1^1/0_0^0$ of TRN(OH).[3] This ratio significantly depends on the expansion conditions, as is clear from Figure 2. The intensity of the band at $\Delta\nu = -54.1$ cm^{-1} (26 963.6 cm^{-1}) considerably decreased under the colder conditions, indicating that this band is the $0_0^0H_1^1$ transition of the 1:1 complex. The band at $\Delta\nu = -54.1$ cm^{-1} was assigned to the intermolecular vibrational mode t_{z0}^1 by Sinha et al.,[23] where t_z indicates the torsion around the out-of-plane z axis. A lot of weak bands are overlapping in the region $\Delta\nu = -55$ to -20 cm^{-1}, which have been separated in the hole-burning spectra shown in the following section.

We have extensively searched for the higher-wavenumber tunneling doublet components $0_0^0H_1^1$ in the spectra of TRN-(OH)−$(N_2)_2$ [I] and TRN(OH)−$(N_2)_2$ [II]. The intensity of the band at $\Delta\nu = -124.1$ cm^{-1} assigned previously as the $0_0^0H_1^1$ transition of TRN(OH)−$(N_2)_2$ [I][23] exhibits no significant temperature dependence. The separation between the 0_0^0 and $0_0^0H_1^1$ transitions of isomer I may be too small to be resolved. Similarly, no $0_0^0H_1^1$ transition is resolved in the spectrum of isomer II.

In order to confirm the above assignment of the $0_0^0H_1^1$ transition of the 1:1 complex and a very small separation (<0.5 cm^{-1}) between the 0_0^0 and $0_0^0H_1^1$ transitions of the 1:2 complexes, we measured the fluorescence excitation spectrum of TRN(OD)−N_2. If the tunneling splitting of the OH species is

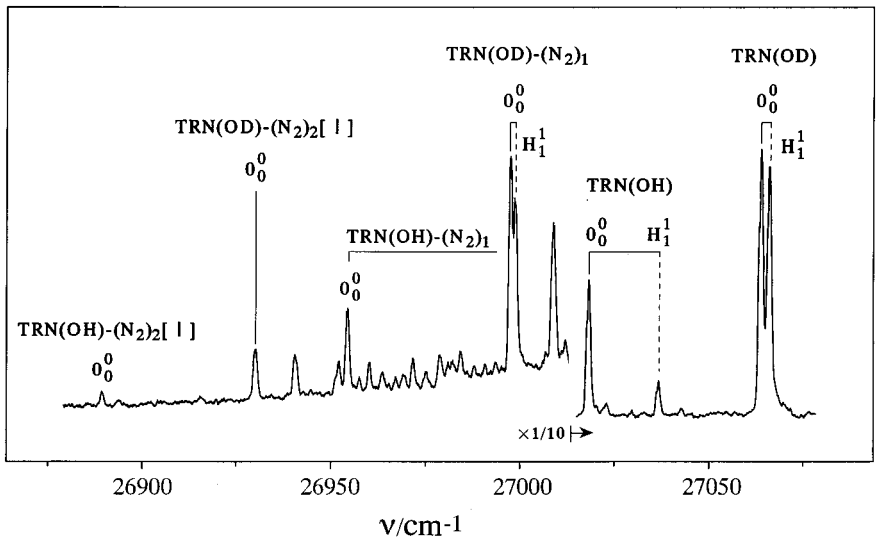

Figure 3. Fluorescence excitation spectra of TRN(OD)−N_2. The experimental conditions were P_0 = 3.5 atm and X/D = 80.

TABLE 1: Wavenumbers and Assignment in the Fluorescence Excitation Spectrum of TRN−$(N_2)_n$ (n = 1, 2)

	this work		Sinha et al.[a]	
molecule	wave-number[b]	assign-ment	wave-number[b]	assign-ment
TRN(OH)−$(N_2)_2$ [I]	26 888.7	0_0^0	26 885.5	0_0^0
			26 891.5	0_0^0 H_1^1
TRN(OH)−$(N_2)_2$ [II]	26 959.8	0_0^0		
TRN(OH)−$(N_2)_1$	26 953.9	0_0^0	26 952.0	0_0^0
	26 963.6	0_0^0 H_1^1	26 958.0	0_0^0 H_1^1
TRN(OH)	27 017.7	0_0^0	27 017.5	0_0^0
	27 036.6	0_0^0 H_1^1	27 036.9	0_0^0 H_1^1
TRN(OD)−$(N_2)_2$ [I]	26 929.5	0_0^0	26 932.0	0_0^0
TRN(OD)−$(N_2)_1$	26 997.1	0_0^0	26 997.0	0_0^0
	26 998.0	0_0^0 H_1^1		
TRN(OD)	27 066.0	0_0^0	27 066.0	0_0^0
	27 068.2	0_0^0 H_1^1	27 068.1	0_0^0 H_1^1

[a] Ref 24. [b] Uncertainties are ±0.5 cm^{-1}.

larger than 6 cm^{-1}, the corresponding splitting in the OD species is expected to be ≥0.6 cm^{-1}. It is possible to detect the splitting of about 0.6 cm^{-1} in our resolution. In Figure 3, the band origin of TRN(OD)−$(N_2)_1$ splits into a doublet with a very small separation of 0.9 cm^{-1}. The lower- and higher-wavenumber components of the doublet are assigned to the 0_0^0 and $0_0^0H_1^1$ transitions, respectively. The ratio of the 0_0^0 tunneling splitting of TRN(OD)−$(N_2)_1$ to that of TRN(OH)−$(N_2)_1$ is 0.093. This value is within the values (0.092−0.127) for various TRN−M_1 (M = Ar, Kr, Xe, CH_4/CD_4, C_2H_6) complexes.[20,21] The electronic origin band of TRN(OD)−$(N_2)_2$ [I] has a single peak (Figure 3), indicating that the 0_0^0 tunneling splitting is not resolved. The 0_0^0 band of TRN(OD)−$(N_2)_2$ [II] may be buried under the very strong 0_0^0 band of the bare molecule and could not be detected.

It is worth noting that the band at $\Delta\nu$ = −57.8 cm^{-1} (ν = 27 008.2 cm^{-1}) in the spectrum of TRN(OD)−$(N_2)_1$ is strong. Such a strong vibronic band is not observed in TRN(OH)−$(N_2)_1$ shown in Figure 1. This band exhibits no tunneling doublet splitting. The wavenumbers and the assignments in the fluorescence excitation spectra of TRN−$(N_2)_n$ (n = 1−2) are summarized in Table 1.

B. Hole-Burning Spectra of TRN−$(N_2)_n$ (n = 1, 2). The hole-burning spectra obtained by probing the 0_0^0 band of TRN-(OH)−$(N_2)_1$ and the bands at 0_0^0 + 9.7 cm^{-1} and 0_0^0 + 5.9 cm^{-1} are shown in Figures 4b−d together with the excitation spectrum (Figure 4a). A comparison of the three hole-burning spectra with the excitation spectrum reveals that the excitation spectrum consists of three band systems that are heavily overlapped one another. The bands with frequencies 18, 25, and 29 cm^{-1} are observed in both Figures 4b and 4c, which are denoted by α′, β′, γ′ and α, β, γ in Figures 4b and 4c, respectively, suggesting that two systems in Figures 4b and 4c

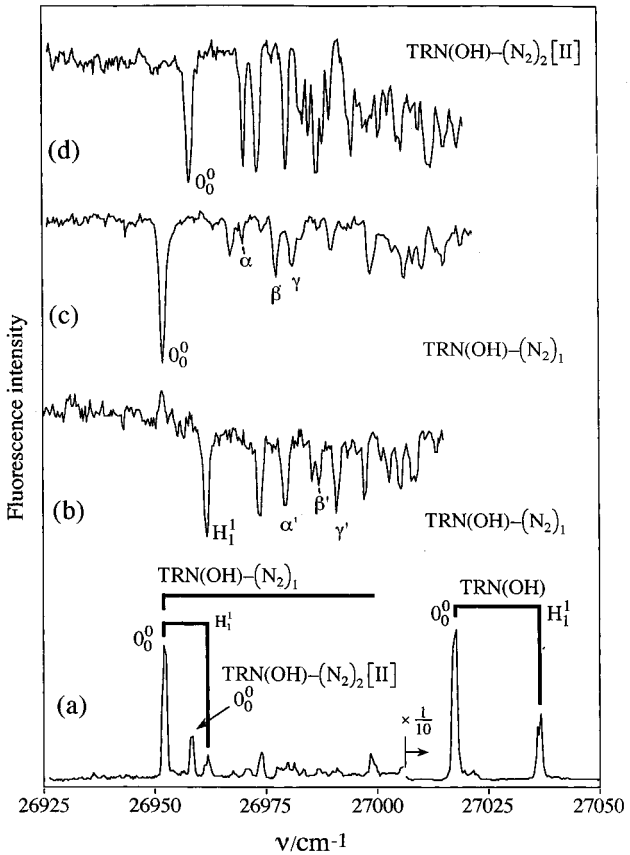

Figure 4. Hole-burning spectra of TRN(OH)−N_2 measured by probing the 0_0^0 + 9.7 cm^{-1} band of TRN(OH)−$(N_2)_1$ (b), the 0_0^0 band (c), and the 0_0^0 + 5.9 cm^{-1} band (d) in the fluorescence excitation spectrum (a). The experimental conditions were P_0 = 2.5 atm, X/D = 40 for (b) and P_0 = 3.0 atm, X/D = 60 for (c) and (d).

originate from the high-wavenumber and low-wavenumber tunneling doublet components, consistent with the assignments of the 0_0^0 and $0_0^0H_1^1$ transitions in the excitation spectrum of TRN(OH)−$(N_2)_1$. The vibrational distribution in Figure 4d is much more congested than those in Figures 4b and 4c. This may be due to the increase in the vibrational degrees of freedom by the solvation of additional N_2. We concluded that the band at $0_0^0 + 5.9$ cm^{-1} is not a vibronic band of TRN(OH)−$(N_2)_1$ but the 0_0^0 band of TRN(OH)−$(N_2)_2$ [II] on the basis of the results from the hole-burning and fluorescence excitation spectra.

The intensity distribution and vibrational frequencies of a few bands are different between Figures 4b and 4c. A similar trend was observed in the hole-burning spectrum of TRN(OH)−Kr_1.[26] In addition to the $b_{y0}^1H_1^1$, $b_{y0}^2H_1^1$, and $s_{z0}^1H_1^1$ transitions observed in the fluorescence excitation spectrum,[19,20] the $b_{x0}^1H_1^1$ and $b_{x0}^1b_{x0}^1H_1^1$ transitions were detected when the $0_0^0H_1^1$ transition was probed. The notations b_x and b_y are the bending modes along the short and long axes of TRN, respectively, while s_z is the stretching mode, and z is perpendicular to the molecular plane of TRN. The b_{x0}^1 and $b_{x0}^1b_{y0}^1$ transitions were absent in the hole-burning spectrum measured by probing the 0_0^0 band, probably due to poor Franck−Condon overlapping between the S_0 and S_1 states. These observations suggest that the vibrational relaxation rates are larger for the $b_x^1H^1$ and $b_x^1b_y^1H^1$ levels than those for the b_x^1 and $b_x^1b_y^1$ levels. By analogy, we infer that the transitions with very small Franck−Condon factors and/or low fluorescence quantum yields are observed in Figures 4b−d.

C. Fluorescence Excitation and Hole-Burning Spectra of TRN−CO. The fluorescence excitation spectrum of TRN(OH)−CO is shown in Figure 5, which is very similar to that reported previously.[24] Sinha et al.[24] assigned the bands at $\Delta\nu = -53.4$ cm^{-1} ($\nu = 26\,964.3$ cm^{-1}) and -78.1 cm^{-1} ($\nu = 26\,939.6$ cm^{-1}) to the 0_0^0 bands of TRN(OH)−$(CO)_1$ [I] and TRN(OD)−$(CO)_1$ [II], respectively. In order to examine the observation of two isomers I and II, we have measured the hole-burning spectrum. Figure 6 shows the hole-burning spectrum measured by probing the strongest band at $\nu = 26\,964.3$ cm^{-1}. It should be noted that the vibronic pattern in the hole-burning spectrum is essentially the same as that in the fluorescence excitation spectrum, and both the bands at -53.4 and -78.1 cm^{-1} are clearly observed. This result unambiguously indicates that no band due to the second isomer is observed in the fluorescence excitation spectrum, inconsistent with the assignment of Sinha et al.[24] The band at $\Delta\nu = -78.1$ cm^{-1} is the 0_0^0 band of TRN(OH)−$(CO)_1$, but the band at $\Delta\nu = -53.4$ cm^{-1} is a vibronic band of TRN−(OH)−$(CO)_1$. No temperature dependence was observed for the intensities of vibronic bands in Figure 5, indicating that the tunneling doublet splittings of vibronic bands are too small to resolve (0.5 cm^{-1}) or completely quenched. We attempted to observe the bands of TRN(OH)−$(CO)_2$; however, no prominent band was observed in the wavenumber region lower than the 0_0^0 band of TRN(OH)−$(CO)_1$.

Figure 7 displays the fluorescence excitation spectrum of TRN(OD)−$(CO)_1$ measured for further confirmation of very small tunneling splitting in TRN(OH)−$(CO)_1$ and to investigate the spectral shift of the electronic origin band. The 0_0^0 band of TRN(OD)−$(CO)_1$ is observed at 26 975.2 cm^{-1} as a shoulder of a vibronic band of TRN(OH)−$(CO)_1$ at 26 973.8 cm^{-1} in Figure 5. This value provides the OH/OD spectral shift of the 0_0^0 band to be 35.6 cm^{-1}.

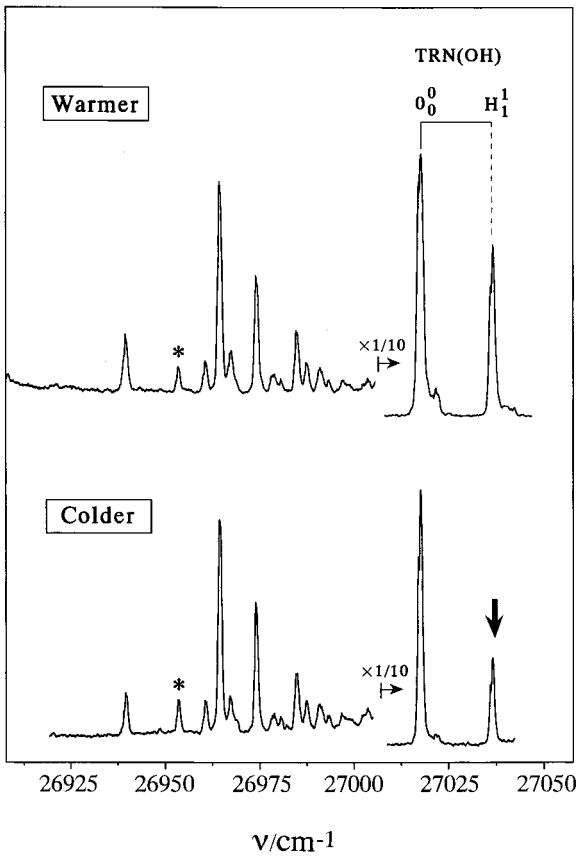

Figure 5. Fluorescence excitation spectra of TRN(OH)−CO. The upper and lower spectra were measured under warmer and colder expansion conditions, respectively. The band marked by the asterisk is due to TRN(OH)−N_2. The experimental conditions were $P_0 = 3.5$ atm and X/D = 40 and $P_0 = 3.5$ atm and X/D = 80, for the upper and lower spectra, respectively.

4. Discussion

A. Spectral Shift and Structures. The microscopic red-shifts of several TRN−M_n ($n = 1, 2$) complexes are plotted in Figure 8 against the average polarizaibility of M. These data provide information on the binding energies and structures of the vdW complexes. The red-shifts of TRN(OH)−$(N_2)_1$ and TRN−$(CO)_1$ are larger than those of the rare gas atoms. However, if we plot the red-shifts against the parallel component of the polarizabilities, 2.60 and 2.38 Å^3 for N_2 and CO, respectively, the shifts for the N_2 and CO complexes are closer to the linear line drawn for the red-shifts of the complexes for TRN with rare gas atoms.

The OH/OD isotope shifts of the 0_0^0 bands for TRN−$(N_2)_1$ and TRN−$(CO)_1$ are 43.2 and 35.6 cm^{-1}, respectively. We obtained a 38.3 cm^{-1} OH/OD shift for TRN−$(N_2)_1$ by subtracting the contribution of the tunneling splitting of TRN(OH)−N_2 (9.7/2 cm^{-1}) from 43.2 cm^{-1}. Thus, the OH/OD isotope shifts are very similar in the two complexes, suggesting that a similarity exists in the structures of TRN−$(N_2)_1$ and TRN−$(CO)_1$. By combining the OH/OD isotope shifts with the red-shifts in Figure 8, we concluded that CO as well as N_2 is located above the ring of TRN. Sinha et al.[24] reported the observation of two isomers for TRN−$(CO)_1$; the carbon atom of CO is hydrogen bonded with the hydroxy proton of TRN in isomer I, and the CO is located above the tropolone ring in isomer II. But the hole-burning spectrum ruled out this possibility.

Recently, a very large red-shift (-351 cm^{-1}) was observed in the S_1-S_0 transition of aniline−$(CO)_1$.[27] The measurement

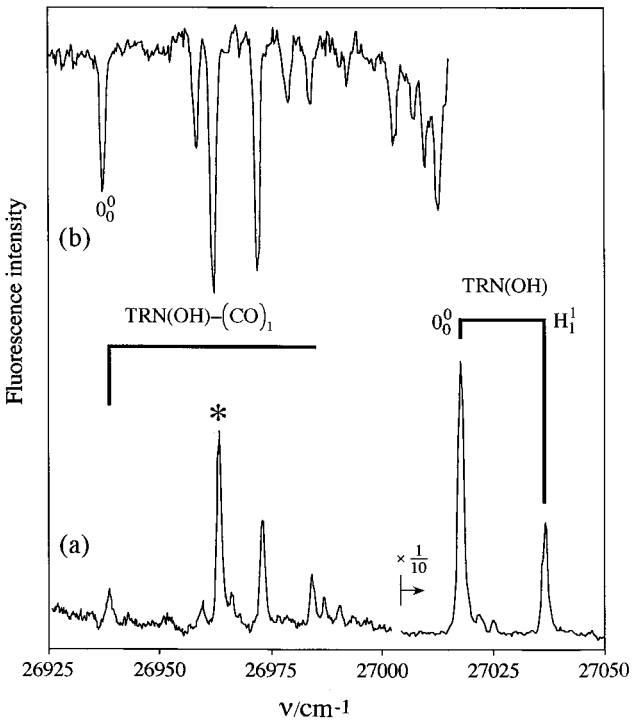

Figure 6. Hole-burning spectrum of TRN(OH)−CO measured by probing the band with the asterisk (b) in the fluorescence excitation spectrum (a). The bands with frequencies 18, 25, and 29 cm^{-1} are observed in both Figures 4b and 4c, which are denoted by α', β', γ' and α, β, γ in Figures 4b and 4c, respectively. The experimental conditions were $P_0 = 3.0$ atm and X/D = 60.

of the NH stretching frequency obtained from the infrared spectrum suggested that CO is located above the benzene ring. The red-shift of the S_1-S_0 transition for carbazole−$(CO)_1$ was measured to be −162.7 cm^{-1}.[28] The red-shifts of aniline−$(N_2)_1$[29,30] and carbazole−$(N_2)_1$[28] are −130 and −93.0 cm^{-1}, respectively. These values are much smaller than the corresponding ones of the CO complexes, suggesting that the interactions of a highly polar molecule with CO are stronger than the complexes of weakly polar or nonpolar molecules with CO such as benzene−$(CO)_1$[31] due to the presence of the electrostatic interactions. Thus, a much larger red-shift for the CO complex than the N_2 complex seems to be a feature in the vdW complexes of a polar chromophore molecule with CO, and the larger red-shift for TRN(OH)−$(CO)_1$ than that for TRN(OH)−$(N_2)_1$ is not unusual.

The red-shift of TRN(OH)−$(N_2)_2$ [I] is almost twice that of TRN(OH)−$(N_2)_1$, suggesting that two N_2 molecules occupy equivalent positions. Two N_2 molecules must be located above and below the tropolone ring in TRN(OH)−$(N_2)_2$ [I], whereas two N_2 molecules may be bonded on the same side of the tropolone ring in TRN(OH)−$(N_2)_2$ [II] based on the much smaller red-shift. Similar structures have been proposed for the TRN−$(C_2H_6)_2$ and benzene−M_2 (M = C_2H_6, C_3H_8) complexes.[32]

On the basis of the structures predicted from the experimental findings we have calculated the conformations of TRN(OH)−$(N_2)_n$ (n = 1, 2) and TRN(OH)−$(CO)_1$ in the S_0 state by using Lennard-Jones 6−12 atom−atom pair potentials and a Lennard-Jones 6−12−1 potentials, respectively, following the method developed by Nowak et al.[32] The atom−atom interaction parameters used in the calculation were obtained from Nemethy et al.[33] The C_s structure of TRN(OH) was obtained from ab initio calculations at the RHF/6-31G** level,[34] which was used to fix the molecular framework. The dispersion interaction is a principal interaction between TRN and N_2/CO. This interaction will be stronger in the excited state, as the π system of TRN will be more delocalized and thus more polarizable. The calculated stable conformers for TRN(OH)−$(N_2)_n$ (n = 1, 2) and TRN(OH)−$(CO)_1$ are illustrated in Figures 9a and 9b, respectively.

In TRN(OH)−$(N_2)_1$ the N_2 molecule (conformer A) is located 3.25 Å above the tropolone ring. The direction of N_2 is nearly parallel to the direction of the permanent dipole moment of TRN, which is nearly parallel to the direction of the C═O double bond. The calculated binding energy (621 cm^{-1}) is in good agreement with a value 620 cm^{-1} reported previously.[23]

The calculations suggest that conformer B has a symmetric sandwich structure, in which two N_2 molecules are located on the opposite sides of the molecular plane of TRN(OH). The binding energy for conformer B is estimated to be 1249 cm^{-1}. This value is almost twice that for A. The observed red-shift for isomer I is also twice that of conformer A. Therefore, conformer B may correspond to TRN(OH)−$(N_2)_2$ [I]. In contrast with conformer B, two N_2 molecules are located on the same side of the molecular plane of TRN(OH) in conformer C, in which one N_2 is located over the seven-membered ring, whereas the other N_2 is located at the position close the O···H−O moiety. The observed TRN(OH)−$(N_2)_2$ [II] may correspond to conformer C. The much smaller redshift of TRN(OH)−$(N_2)_2$ [II] as compared to that of TRN(OH)−$(N_2)_2$ [I] can be explained by poor overlap of the π system of TRN with the orbitals of N_2 close to the O···H−O moiety, resulting in smaller binding energy in the S_1 state for conformer C than for conformer B. The binding energy for conformer B (1249 cm^{-1}) in the S_0 state is only slightly larger than that for conformer C (1193 cm^{-1}). The similarity in the calculated binding energies for the two conformers is consistent with the observation of isomers I and II under the same expansion conditions.

Two stable conformers A and B are obtained for TRN(OH)−$(CO)_1$ from Lennard-Jones potential calculations as illustrated in Figure 9b. The CO molecule is located 3.13-3.15 Å above the plane of TRN(OH) in conformers A and B. The positions of CO are significantly different between the two conformers. The oxygen atom of CO is closer to the O···H−O moiety than the carbon atom in conformer A, whereas the oxygen atom is located far from the O···H−O moiety in conformer B. The binding energies are similar for conformers A (772 cm^{-1}) and B (753 cm^{-1}). The energy barrier for the rotation of CO in the plane of S_0 TRN(OH) was calculated to be about 30 cm^{-1}. Thus, Lennard-Jones potential calculations can roughly predict the structure of TRN(OH)−$(CO)_1$; that is, the CO molecule is located above the seven-membered ring of TRN(OH).

B. Tunneling Splittings. The 0_0^0 tunneling splittings $|\Delta_0' - \Delta_0''|$ of TRN−$(N_2)_n$ (n = 1, 2) and TRN−$(CO)_1$ determined in the present work are listed in Table 2 together with those of various TRN−M_n complexes reported previously.[19−21] The decreases or increases in the tunneling splitting in TRN−M_n must be due to the changes in the tunneling doublet splitting in the zero-point level of the S_1 state, Δ_0', because the corresponding value in the S_0 state of the bare molecule, Δ_0'', is very small (0.99 cm^{-1}).[35] The 0_0^0 tunneling doublet splitting was observed only in TRN−$(N_2)_1$ among the TRN−$(N_2)_n$ (n = 1, 2) and TRN−$(CO)_1$ complexes. The $|\Delta_0' - \Delta_0''|$ values of TRN(OH)−$(N_2)_1$ and TRN(OD)−$(N_2)_1$ are 9.7 and 0.9 cm^{-1}, respectively. The $|\Delta_0' - \Delta_0''|$ value of TRN(OH)−$(N_2)_1$ is about half that of TRN(OH). The 0_0^0 tunneling splitting is almost completely quenched in TRN(OH)−$(N_2)_2$ [II].

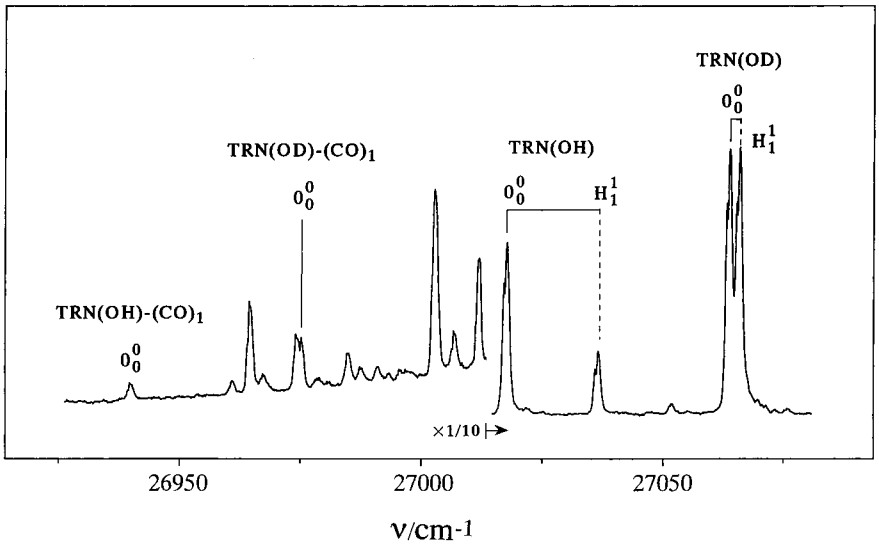

Figure 7. Fluorescence excitation spectra of TRN(OD)−CO. The experimental conditions were $P_0 = 3.5$ atm and X/D = 80.

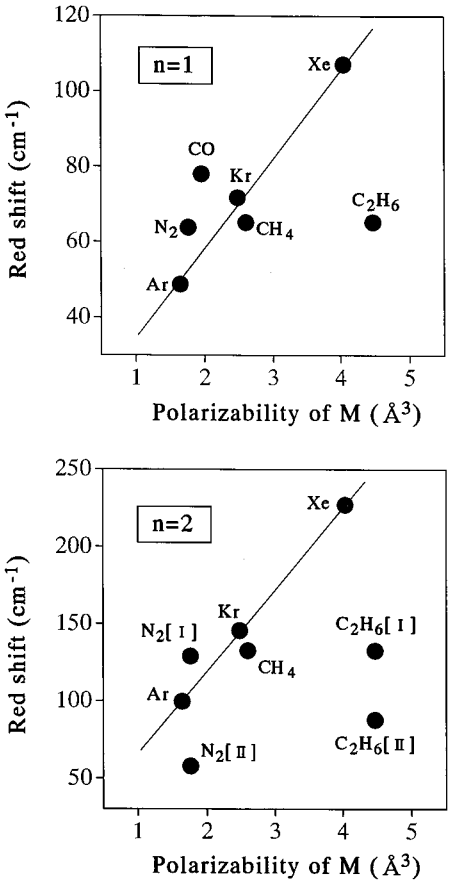

Figure 8. The microscopic red-shifts against the polarizability of M. The upper and lower figures are for TRN−M_1 and TRN−M_2, respectively.

The $|\Delta_0' - \Delta_0''|$ values of TRN(OH)−Rg (Rg = Ar, Kr, Xe)[19] are very similar to that of TRN, although the binding energies for TRN(OH)−Kr_1 and TRN(OH)−Xe_1 are much larger than those for TRN(OH)−$(N_2)_1$ and TRN(OH)−$(CO)_1$. These results suggest that the magnitude of the binding energy is not a dominant factor for the changes in the tunneling splitting. An important factor influencing the tunneling PESs must be related to the anisotropy of the molecular polarizability of M from substantial decreases in $|\Delta_0' - \Delta_0''|$ of TRN(OH)−M_1 (M = N_2, CO, C_2H_6, C_3H_8). The decreases in the tunneling splittings of TRN−M_1 (M = N_2, CO) are ascribed to the coupling of the intermolecular vibrations with the intramolecular vibrations. This coupling may provide the following two effects on the symmetric PES of TRN along the tunneling coordinate: (i) The coupling makes the plane of TRN nonplanar, which increases the height of the tunneling potential energy barrier and/or tunneling distance. (ii) Asymmetric interactions lower the effective symmetry of TRN in the transition state, and the tunneling PES along the tunneling coordinate may be slightly asymmetric. No TRN−M_1 (M = molecule) complex that exhibits an increase in the tunneling splitting has been observed, while the tunneling splittings are increased in TRN−Kr_2 and TRN−Xe_2. In these complexes, TRN may be more planar in the S_1 state as compared to the bare molecule, leading to a lower potential energy barrier to tunneling. In contrast, the decrease in the planarity and/or the increase in the O···O distance may substantially increase the tunneling potential energy barrier.The intramolecular modes which couple with the intermolecular mode(s) may depend on the geometry of TRN−M_1. Since the rate of proton transfer in the S_1 state of TRN(OH) is much faster than that of the rotation of M, the geometries of TRN−M_1 before and after the proton transfer may be different. This difference may become larger with increasing the height of the potential barrier for rotating M on the plane of TRN. Lennard-Jones atom−atom pair potential calculations suggest that this barrier is larger in the S_0 state of TRN−$(CO)_1$ than in TRN−$(N_2)_1$. The asymmetric structures before and after proton transfer may significantly change the tunneling PES. Takada and Nakamura pointed out that the asymmetry of PES in the transition state significantly decreases the tunneling splitting by calculating PESs of TRN in the S_0 state.[11]

The smaller 0_0^0 tunneling splittings of TRN−$(CO)_1$ than that of TRN−$(N_2)_1$ could be explained by the above two effects. The potential energy barrier for rotating CO on the plane of TRN is predicted to be larger than that for rotating N_2. The N_2 molecule is delocalized in the plane of TRN in TRN(OH)−$(N_2)_1$. The change in the vibronic structure upon deuteration suggests that N_2 may tend to localize in TRN(OD)−$(N_2)_1$. The degree of delocalization may be more decreased in TRN(OH)−CO. A similar effect on the localization of the adduct has been observed in the TRN−$(CH_4/CD_4)_1$ complexes. The 0_0^0 tunneling splitting of TRN−$(CD_4)_1$ is smaller than that of TRN−$(CH_4)_1$. This H/D isotope effect on the tunneling splitting cannot

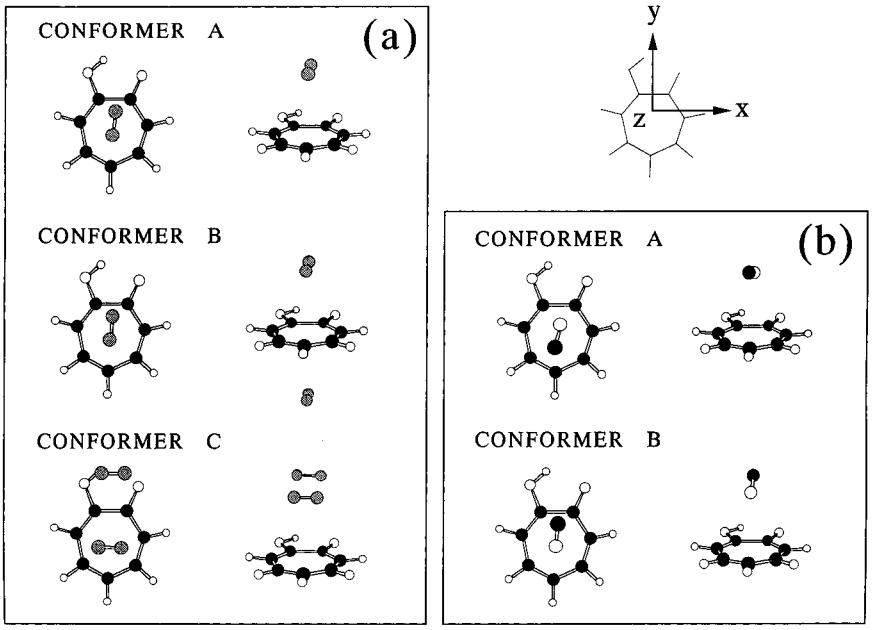

Figure 9. Top (left) and side (right) views of the calculated minimum energy structures for TRN−$(N_2)_n$ (n = 1, 2) and TRN−$(CO)_1$ illustrated in (a) and (b), respectively.

TABLE 2: Tunneling Splittings $|\Delta_0' - \Delta_0''|$ (cm^{-1}) of TRN−M_n

TRN(OH)−M_n	$\lvert\Delta_0' - \Delta_0''\rvert$/ cm^{-1}	TRN(OD)−M_n	$\lvert\Delta_0' - \Delta_0''\rvert$/ cm^{-1}
$(N_2)_1$[a]	9.7	$(N_2)_1$[a]	0.9
$(CO)_1$[a]	<0.5	$(CO)_1$[a]	<0.5
Ar_1[b]	18.0		
Kr_1[b]	18.3	Kr_1[b]	2.0
Xe_1[b]	17.3	Xe_1[b]	2.2
$(CH_4)_1$[c]	16.2	$(CH_4)_1$[c]	1.8
$(CD_4)_1$[c]	14.6	$(CD_4)_1$[c]	1.6
$(C_2H_6)_1$[d]	12.0	$(C_2H_6)_1$[d]	1.4
$(C_3H_8)_1$[d]	13.9	$(C_3H_8)_1$[d]	1.3
$(N_2)_2$ [I][a]	<0.5	$(N_2)_2$ [I][a]	<0.5
$(N_2)_2$ [II][a]	<0.5		
Ar_2[d]	18.8	Ar_2[d]	2.2
Kr_2[d]	19.7	Kr_2[d]	2.1
Xe_2[d]	20.2		
$(CH_4)_2$[d]	13.9	$(CH_4)_2$[d]	1.6
$(C_2H_6)_2$ [I][d]	9.0	$(C_2H_6)_2$ [I][d]	0.8
$(C_2H_6)_2$ [II][d]	<0.5	$(C_2H_6)_2$ [II][d]	<0.5
$(C_3H_8)_2$[d]	<0.5	$(C_3H_8)_2$[d]	<0.5

[a] This work. [b] Ref 19. [c] Ref 20. [d] Ref 21.

be explained by the intermolecular interactions involving the dispersive, Coulomb, and dipole−induced−dipole interactions for the same configurations of the TRN−$(CH_4/CD_4)_1$ complexes. One explanation is the vibrational tunneling effect[36] on the rotation of CH_4 above the molecular plane of TRN. When the potential energy barrier exists for the rotation of CH_4/CD_4, CD_4 will be preferentially trapped by a potential surface. Therefore, the positions of the H/D atoms may be asymmetric in TRN−$(CH_4/CD_4)_1$.

The strength of the coupling between the intermolecular vibrations and the intramolecular vibrations is larger in TRN−$(N_2)_2$ than in TRN−$(N_2)_1$. When one N_2 molecule is located at the position close to the O···H−O moiety in TRN−$(N_2)_2$ [II], as suggested by the calculations, the motion of this N_2 molecule may couple with the motions of the hydroxy proton or the oxygen atoms. This coupling will significantly change the proton-transfer coordinate and/or increase the O···O distance, leading to much smaller tunneling splitting. The 0_0^0 tunnelings of TRN−$(C_2H_6)_2$ [II] and TRN$(C_3H_8)_2$,[21] which have conformations similar to TRN−$(N_2)_2$ [II], are less than 0.5 cm^{-1}, consistent with the explanation for the quenching of the tunneling splitting of TRN−$(N_2)_2$ [II]. In general, the 0_0^0 tunneling splitting of TRN−M_2 is smaller than that of TRN−M_1 except for TRN−Rg_2. This implies that two molecules act in concert during proton transfer.

C. Intermolecular Vibrations. A lot of very weak vibronic bands are observed in the excitation spectrum of TRN(OH)−$(N_2)_1$. These bands are prominently observed in the hole-burning spectrum. The transitions may terminate into the levels due to the intermolecular bending, stretching, and torsion modes in the S_1 state. The torsion mode originates from the rotation of N_2 above the molecular plane of TRN(OH). The intensity distribution in Figure 4b is different from that in Figure 4c, probably due to the difference in the vibrational relaxation rate between the lower- and higher-wavenumber tunneling doublet components in the S_1 state and the Franck−Condon factors. The frequencies of a few vibronic bands in Figure 4b are shifted from those in Figure 4c, implying that the magnitude of the tunneling doublet splitting depends on the excited intermolecular vibrational levels. This result could be compared with the tunneling splittings in the vibrationally excited intermolecular levels of TRN−Rg_1 (Rg = Ar, Kr, Xe) in which the tunneling doublet splittings of vibronic bands are very similar to the 0_0^0 tunneling splitting of the bare molecule. The coupling of the intermolecular vibrations with the intramolecular vibrations must be much larger in TRN−$(N_2)_1$ than in TRN−Rg_1.

It is difficult to make definite assignments for many vibronic transitions of TRN(OH)−$(N_2)_1$ owing to lack of sufficient data on the exact geometry and the intermolecular potentials. The very complicated vibronic structure in the spectrum of TRN-(OH)−$(N_2)_1$ is due to significant delocalization of N_2 in the plane of TRN(OH). The delocalization of N_2 may mix the intermolecular vibrational modes, and a lot of transitions emerge in the spectrum. Such a mixing of the intermolecular modes has been observed in the spectra of TRN(OH)−Rg_1 (Rg = Ar, Kr).

The vibronic pattern in the spectrum of TRN(OH)−$(CO)_1$ is very different from that in TRN(OH)−$(N_2)_1$ and those in the spectra of TRN(OH)−M_1 (M = Rg, CH_4, C_2H_6) complexes

studied previously.[19−21] The electronic origin band is substantially weak in TRN(OH)−$(CO)_1$, whereas the electronic origin band is much stronger than the excited vibronic bands in the spectra of TRN(OH)−M_1 (M = Rg, N_2, CH_4, C_2H_6). The energy barrier for the rotation of CO in the plane of S_0 TRN(OH) was calculated to be about 30 cm^{-1} by Lennard-Jones atom−atom pair potential calculations, which is much larger than the corresponding value (10 cm^{-1}) for TRN(OH)−$(N_2)_1$, preventing rearrangement of CO by the torsional motion during proton transfer. The vibronic pattern in the excitation spectrum suggests the geometry of TRN(OH)−$(CO)_1$ in the S_1 state is very different from that in the S_0 state. Probably, the change in the geometry is due to the interactions of the electric charge on CO with TRN(OH) which may change substantially by photoexcitation.

5. Conclusion

We investigated the structures and proton tunneling in the S_1 states of TRN(OH)−$(N_2)_n$ (n = 1, 2) and TRN(OH)−$(CO)_1$ van der Waals complexes and their deuterated species. Hole-burning spectroscopy has been successfully applied to distinguish the structural isomers and to separate transitions between the lower-wavenumber and higher-wavenumber tunneling doublet components of the same species. Only one species was observed for TRN(OH)−$(N_2)_1$ and TRN(OH)−$(CO)_1$, while two stable isomers are identified for TRN−$(N_2)_2$. The 0_0^0 tunneling splittings of TRN(OH)−$(N_2)_1$ and TRN(OD)−$(N_2)_1$ are about half that of the corresponding bare molecule. The 0_0^0 tunneling splittings are not resolved in TRN(OH)−$(CO)_1$ and TRN−$(N_2)_2$-[II]. The CO molecule more strongly interacts with TRN than the N_2 molecule, although the two molecules are isoelectronic. The electric charge on the CO molecule substantially influences the intermolecular interactions and influences the localization in the S_1 state of TRN(OH)−$(CO)_1$. The origins of the decreases in the tunneling splittings in the observed complexes have been discussed on the basis of the observed spectral shifts, vibronic patterns in the spectra, and the conformations obtained from Lennard-Jones atom−atom pair potential calculations. The N_2 or CO molecules are predicted to be located on the seven-membered ring of TRN in the 1:1 complexes. Two N_2 molecules are located on the opposite side of the seven-membered ring of TRN in TRN−$(N_2)_2$ [I]. In TRN−$(N_2)_2$ [II] one N_2 molecule is suggested to be located on the plane nearly parallel to the plane of the O···H−O moiety. The intermolecular vibrations may directly couple with the proton-transfer coordinate and increase the height of the potential energy barrier to proton transfer in TRN−$(N_2)_2$ [II]. In the other species studied in the present work, the intermolecular vibrations couple with the intramolecular vibrations of TRN, which may couple with the proton-transfer mode and increase the potential energy barrier.

The vibrational relaxation has been suggested to be very fast in the vibronic levels of the S_1 states of TRN(OH)−$(N_2)_n$ (n = 1, 2) and TRN(OH)−$(CO)_1$; that must be the reason why higher vibronic levels (>70 cm^{-1}) have not been observed or are very weak in the fluorescence excitation spectra of the TRN−M_n complexes studied previously.

Acknowledgment. This work was partly supported by Grants-in-Aid for Scientific Research on Priority Area "Quantum Tunneling of group of Atoms as Systems with Many Degrees of Freedom" Area No. 271/09622230 from the Ministry of Education, Science, Sports and Culture of Japan.

References and Notes

(1) Rossetti, R.; Rayford, R.; Haddon, R. C.; Brus, L. E. *J. Am. Chem. Soc.* **1981**, *103*, 4303.
(2) Alves, A. C. P.; Hollas, J. M.; Musa, H.; Ridley, T. *J. Mol. Spectrosc.* **1985**, *109*, 99.
(3) Tomioka, Y.; Ito, M.; Mikami, N. *J. Phys. Chem.* **1983**, *87*, 4401.
(4) Redington, R.; Chen. Y.; Scherer, G. J.; Field, R. W. *J. Chem. Phys.* **1988**, *88*, 627.
(5) Sekiya, H.; Nagashima, Y.; Nishimura, Y. *Bull. Chem. Soc.* **1989**, *62*, 3229.
(6) Sekiya, H.; Nagashima, Y.; Nishimura, Y. *J. Chem. Phys.* **1990**, *92*, 5761.
(7) Sekiya, H.; Nagashima, Y.; Tsuji, T.; Nishimura, Y.; Mori, A.; Takeshita, H. *J. Phys. Chem.* **1991**, *95*, 10311.
(8) Frost, R. K.; Hagemeister, F. C.; Arrington, C. A.; Zwier, T. S. *J. Chem. Phys.* **1996**, *105*, 2595.
(9) Redington, R. L. *J. Chem. Phys.* **1990**, *92*, 6447.
(10) Vener, M. V.; Scheiner, S.; Sokolov, N. D. *J. Chem. Phys.* **1994**, *101*, 9755.
(11) Takada, S.; Nakamura H. *J. Chem. Phys.* **1995**, *102*, 3997.
(12) Paz, J. J.; Moreno, M.; Lluck, J. *J. Chem. Phys.* **1995**, *103*, 353.
(13) Rossetti, R.; Haddon, R. C.; Brus, L. E. *J. Am. Chem. Soc.* **1980**, *102*, 6913.
(14) Bondybey, V. E.; Haddon, R. C.; English, J. H. *J. Chem. Phys.* **1984**, *80*, 5432.
(15) Bondybey, V. E.; Haddon, R. C.; Rezepis, P. M. *J. Am. Chem. Soc.* **1984**, *106*, 5969.
(16) Ozeki, H.; Takahashi, M.; Okuyama, K.; Kimura, K. *J. Chem. Phys.* **1993**, *99*, 56.
(17) Sekiya, H.; Nakano, N.; Nishi, K.; Hamabe, H.; Sawada, T.; Tashiro, M.; Nishimura, Y. *Chem. Lett.* **1995**, 893.
(18) For example: Buntis, T. *Proton Transfer in Hydrogen-Bonded Systems*; Plenum Press: New York and London, 1992.
(19) Sekiya, H.; Nakajima, T.; Ujita, H.; Tsuji, T.; Ito, S.; Nishimura, Y. *Chem. Phys. Lett.* **1993**, *215*, 499.
(20) Sekiya, H.; Hamabe, H.; Nakajima, T.; Mori, A.; Takeshita, H.; Nishimura, Y. *Chem. Phys. Lett.* **1994**, *224*, 563.
(21) Sekiya, H.; Hamabe, H.; Ujita, H.; Nakano, N.; Nishimura, Y. *J. Chem. Phys.* **1995**, *103*, 3895.
(22) Landolt-Bornstein, *Zahelenwerte und Funkutionen*; Springer Press: Berlin, 1962; pp 509−512.
(23) Sinha, H. K.; Steer, R. P. *Chem. Phys. Lett.* **1995**, *241*, 328.
(24) Sinha, H. K.; MacKenzie, V. J.; Steer, R. P. *Chem. Phys.* **1996**, *213*, 397.
(25) Hamabe, H.; Sekiya, N.; Nakano, H.; Nishi, K.; Nishimura Y. *Chem. Phys. Lett.*, in press.
(26) Fukuchi, T.; Nishi, K; Nishi, N.; Hamabe, H.; Nishimura, Y.; Sekiya, H. To be published.
(27) Jackel, G. J.; Schmid, R.; Jones, H.; Nakanaga, T.; Takeo, H. *Chem. Phys.* **1977**, *215*, 291.
(28) Burgi, T.; Droz, T.; Leutweyler, S. *J. Chem. Phys.* **1995**, *103*, 4035.
(29) Yamanouchi, K.; Isogai, S.; Tsuchiya, S. *J. Mol. Struct.* **1986**, *146*, 349.
(30) Hineman, M. F.; Kim, S. K.; Bernstein, E. R.; Kelley, D. F. *J. Chem. Phys.* **1992**, *96*, 4905.
(31) Schauer, M.; Bernstein, E. R. *J. Chem. Phys.* **1985**, *82*, 726.
(32) Nowak, R.; Menapace, J. A.; Bernstein, E. R. *J. Chem. Phys.* **1988**, *89*, 309; Wanna, J.; Menapace, J.A.; Bernstein, E. R. *J. Chem. Phys.* **1986**, *85*, 1795.
(33) Nemethy, G.; Pottle, M. S.; Scheraga, H. A. *J. Phys. Chem.* **1983**, *87*, 1883.
(34) Nishi, K.; Ujita, H.; Sekiya, H.; Hamabe, H.; Nishimura Y. Unpublished results.
(35) Tanaka, K.; Honjo, H.; Tanaka, T.; Kouguchi, H.; Ohshima, Y.; Endo Y. In *Proceedings of the International Symposium on Molecular Spectroscopy*; Ohio State University: Columbus, OH, 1992.
(36) Wittmeyer, S. A.; Troxler, T.; Topp, M. R. *J. Phys. Chem.* **1993**, *97*, 10613.